Article

Probing the Role of Axial Methionine in the Blue Copper Center of Azurin with Unnatural Amino Acids

Steven M. Berry, Martina Ralle, Donald W. Low, Ninian J. Blackburn, and Yi Lu

J. Am. Chem. Soc., **2003**, 125 (29), 8760-8768• DOI: 10.1021/ja029699u • Publication Date (Web): 25 June 2003

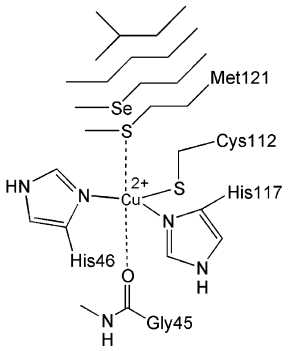

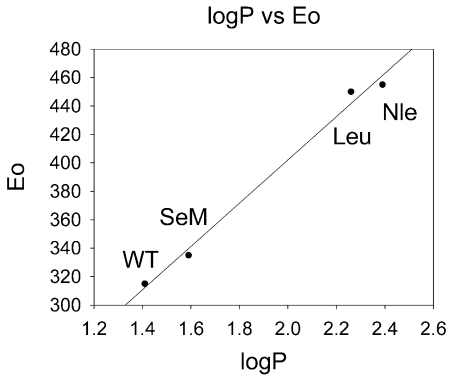

More About This Article

Additional resources and features associated with this article are available within the HTML version:

- Supporting Information
- Links to the 4 articles that cite this article, as of the time of this article download
- Access to high resolution figures
- Links to articles and content related to this article
- Copyright permission to reproduce figures and/or text from this article

View the Full Text HTML

J|A|C|S
ARTICLES
Published on Web 06/25/2003

Probing the Role of Axial Methionine in the Blue Copper Center of Azurin with Unnatural Amino Acids

Steven M. Berry,[†] Martina Ralle,[‡] Donald W. Low,[§] Ninian J. Blackburn,*[,‡] and Yi Lu*[,†]

Contribution from the Department of Chemistry, University of Illinois at Urbana-Champaign, Urbana, Illinois 61801, Department of Biochemistry and Molecular Biology, OGI School of Science & Engineering, Oregon Health & Sciences University, Beaverton, Oregon 97006, and Gryphon Sciences, 250 East Grand Avenue, Suite 90, South San Francisco, California 94080

Received December 11, 2002; E-mail: yi-lu@uiuc.edu; ninian@bmb.ogi.edu

Abstract: Expressed protein ligation was used to replace the axial methionine of the blue copper protein azurin from *Pseudomonas aeruginosa* with unnatural amino acids. The highly conserved methionine121 residue was replaced with the isostructural amino acids norleucine (Nle) and selenomethionine (SeM). The UV−visible absorption, X- and Q-band EPR, and Cu EXAFS spectra of the variants are slightly perturbed from WT. All variants have a predominant S(Cys) to Cu(II) charge transfer band around 625 nm and narrow EPR hyperfine splittings. The Se EXAFS of the M121SeM variant is also reported. In contrast to the small spectral changes, the reduction potentials of M121SeM, M121Leu, and M121Nle are 25, 135, and 140 mV, respectively, higher than that of WT azurin. The use of unnatural amino acids allowed deconvolution of different factors affecting the reduction potentials of the blue copper center. A careful analysis of the WT azurin and its variants obtained in this work showed the large reduction potential variation was linearly correlated with the hydrophobicity of the axial ligand side chains. Therefore, hydrophobicity is the dominant factor in tuning the reduction potentials of blue copper centers by axial ligands.

Introduction

Azurin is an electron-transfer protein involved in bacterial denitrification.[1−10] It is a member of the type 1, or blue copper protein, family known for their intense blue color ($\epsilon_{625\,nm} \approx 5000\ M^{-1}\ cm^{-1}$) and narrow copper hyperfine coupling constant in the parallel region of the electron paramagnetic resonance (EPR) spectrum ($A_{||} \approx 60$ G). The resting state of azurin from *Pseudomonas aeruginosa* contains a redox active Cu(II) ion situated in a pseudo trigonal bipyramidal coordination environment, with His46, His117, and Cys112 on the trigonal base, and a distant carbonyl oxygen from Gly45 and Met121 sulfur in the axial positions (Figure 1).[3,11,12] While a weak covalent Cu(II)−Met121 bond has been implicated, no covalent interaction between the Cu(II) and the carbonyl oxygen of Gly45 has been detected, except a weak ionic interaction.[7,13]

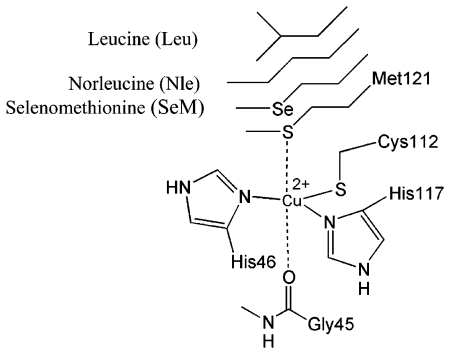

Figure 1. Cartoon depicting the active site of azurin and methionine residue mutations presented in this paper.

The axial methionine (Met121) is highly conserved in blue copper proteins, except in a few cases such as umecyanin, stellacyanin, ceruloplasmin, and laccase.[1,4,9,10] The role of this axial methionine in modulating the structure and function of type 1 copper centers has been investigated through spectroscopic studies,[7,13−15] theoretical calculation,[7,13,16,17] and site-

[†] University of Illinois at Urbana-Champaign.
[‡] Oregon Health & Sciences University.
[§] Gryphon Sciences.

(1) Fee, J. A. *Struct. Bonding* **1975**, *23*, 1−60.
(2) Farver, O.; Pecht, I. In *Copper Proteins*; Spiro, T. G., Ed.; Wiley: New York, 1981; pp 151−192.
(3) Adman, E. T. In *Topics in Molecular and Structural Biology: Metalloproteins*; Harrison, P., Ed.; MacMillan: New York, 1985; Vol. 1, pp 1−42.
(4) Messerschmidt, A. *Struct. Bonding (Berlin)* **1998**, *90*, 37−68.
(5) Malmström, B. G.; Wittung-Stafshede, P. *Coord. Chem. Rev.* **1999**, *185−186*, 127−140.
(6) Gray, H. B.; Malmström, B. G.; Williams, R. J. P. *J. Biol. Inorg. Chem.* **2000**, *5*, 551−559.
(7) Solomon, E. I.; Randall, D. W.; Glaser, T. *Coord. Chem. Rev.* **2000**, *200−202*, 595−632.
(8) Kolczak, U.; Dennison, C.; Messerschmid, A.; Canters, G. W. In *Handbook of Metalloproteins*; Messerschmid, A., Huber, R., Poulos, T., Wieghardt, K., Eds.; Wiley: Chichester, 2001; Vol. 2, pp 1170−1194.
(9) Vila, A. J.; Fernández, C. O. In *Handbook on Metalloproteins*; Bertini, I., Sigel, A., Sigel, H., Eds.; Marcel Dekker: New York, 2001; pp 813−856.
(10) Lu, Y. Comprehensive Coordination Chemistry II: From Biology to Nanotechnology; McCleverty, J. A., Meyer, T. J., Eds.; In *Biocoordination Chemistry*; Que, J. L., Tolman, W. B., Eds.; Elsevier: Oxford, U.K., 2003; Vol. 8, in press.
(11) Adman, E. T. *Adv. Protein Chem.* **1991**, *42*, 145−197.
(12) Nar, H.; Messerschmidt, A.; Huber, R.; van der Kamp, M.; Canters, G. W. *J. Mol. Biol.* **1991**, *221*, 765−772.
(13) Lowery, M. D.; Solomon, E. I. *Inorg. Chim. Acta* **1992**, *198−200*, 233−243.

10.1021/ja029699u CCC: $25.00

directed mutagenesis.[18] For example, mutations of Met121 to natural amino acids in azurin,[19−25] and other type 1 copper proteins,[26−30] have been performed.[19,21,31−33] These axial mutations included about every other naturally occurring amino acid. In addition, certain Met121 mutants have allowed the incorporation of free, exogenous ligands into the axial position.[32,34,35] Furthermore, comparisons across the blue copper protein family have been made. Together, these mutagenesis and comparison studies have yielded a wealth of information regarding the proposed role of the axial ligand. For example, structurally, the methionine is believed to protect the copper ion from interaction with water and exogenous ligands[24,32,35−37] and prevent a large dependence on pH and temperature.[38] Electronically, the axial S(Met)−Cu(II) interaction is proposed to influence the stability of the oxidation states of the copper ion,[39,40] fine-tune the "in-plane" S(Cys)−Cu(II) interaction,[20,41−43] and change the geometry of the blue copper center.[42,44−48] A shorter S(Met)−Cu(II) distance is thought to result in more destabilization of the Cu(II) state, a weaker S(Cys)−Cu(II) bond, and a more tetragonal (or flattened tetrahedral) distortion of the trigonal blue copper center.[49] The influences are manifested by different absorption intensity ratios of A_{460nm} to A_{600nm}, different rhombicity of the EPR signals, different Cu(II)−S(Cys) covalency, and thus different functional properties.[7,44,45,48,50] On the other hand, recent paramagnetic ^{1}H NMR studies on perturbed copper sites have indicated that this strong S(Met)−Cu(II) interaction weakens the S(Cys)−Cu(II) bond only in certain blue copper proteins such as stellacyanin, but not in others such as pseudoazurin and rusticyanin.[51,52] Perhaps the most prominent role of the axial ligand is its ability to tune the reduction potential of the blue copper site, over a range as large as 300 mV.[5,23,29,36] However, it is not the only or the largest influence on the potential. For example, the presence or absence of hydrophobic residues in the secondary coordination sphere of the copper site is also believed to play an important role in tuning the reduction potentials.[6,28,36,53−55]

While many results and several different perspectives have been obtained from the above site-directed mutagenesis and comparison studies, the role of the axial methionine still remains to be clearly defined. One issue commonly associated with site-directed mutagenesis using natural amino acids is that often more than one factor, such as sterics, geometry, and electronic interactions, is changed in one experiment. It is desirable to perform mutagenesis studies on the axial ligand in a blue copper protein framework by changing as few parameters as possible. Replacing the methionine with unnatural amino acids in a systematic manner is an attractive way of achieving such a goal. For example, replacing methionine with norleucine (Nle) allows a measure of the electronic role of the thioether group of Met without changing much of its steric factor. A further advantage of this approach is the ability to introduce new functional groups, such as selenomethionine (SeM), so that the metal−ligand interaction can be decreased or enhanced.

Selenomethionine had been incorporated into azurin from *Pseudomonas aeruginosa* using a Met auxotroph.[39] The protein in the study displayed UV−vis and EPR data slightly perturbed from WT. However, the reduction potential was increased by

(14) Solomon, E. I.; Baldwin, M. J.; Lowery, M. D. *Chem. Rev.* **1992**, *92*, 521−542.
(15) Bertini, I.; Fernandez, C. O.; Karlsson, B. G.; Leckner, J.; Luchinat, C.; Malmström, B. G.; Nersissian, A. M.; Pierattelli, R.; Shipp, E.; Valentine, J. S.; Vila, A. J. *J. Am. Chem. Soc.* **2000**, *122*, 3701−3707.
(16) Ryde, U.; Olsson, M. H. M.; Pierloot, K. *Theor. Comput. Chem.* **2001**, *9*, 1−55.
(17) van Gastel, M.; Coremans, J. W. A.; Sommerdijk, H.; van Hemert, M. C.; Groenen, E. J. J. *J. Am. Chem. Soc.* **2002**, *124*, 2035−2041.
(18) Canters, G. W.; Gilardi, G. *FEBS Lett.* **1993**, *325*, 39−48.
(19) Karlsson, B. G.; Aasa, R.; Malmström, B. G.; Lundberg, L. G. *FEBS Lett.* **1989**, *253*, 99−102.
(20) Karlsson, B. G.; Nordling, M.; Pascher, T.; Tsai, L.-C.; Sjolin, L.; Lundberg, L. G. *Protein Eng.* **1991**, *4*, 343−349.
(21) Chang, T. K.; Iverson, S. A.; Rodrigues, C. G.; Kiser, C. N.; Lew, A. Y. C.; Germanas, J. P.; Richards, J. H. *Proc. Natl. Acad. Sci. U.S.A.* **1991**, *88*, 1325−1329.
(22) Pascher, T.; Karlsson, B. G.; Nordling, M.; Malmström, B. G.; Vänngård, T. *Eur. J. Biochem.* **1993**, *212*, 289−296.
(23) Romero, A.; Hoitink, C. W. G.; Nar, H.; Huber, R.; Messerschmidt, A.; Canters, G. W. *J. Mol. Biol.* **1993**, *229*, 1007−1021.
(24) Kroes, S. J.; Hoitink, C. W. G.; Andrew, C. R.; Ai, J.; Sanders-Loehr, J.; Messerschmidt, A.; Hagen, W. R.; Canters, G. W. *Eur. J. Biochem.* **1996**, *240*, 342−351.
(25) Karlsson, B. G.; Tsai, L.-C.; Nar, H.; Sanders-Loehr, J.; Bonander, N.; Langer, V.; Sjölin, L. *Biochemistry* **1997**, *36*, 4089−4095.
(26) Hibino, T.; Lee, B. H.; Takabe, T. *J. Biochem. (Tokyo)* **1995**, *117*, 101−106.
(27) Shimizu, A.; Sasaki, T.; Kwon, J. H.; Odaka, A.; Satoh, T.; Sakurai, N.; Sakurai, T.; Yamaguchi, S.; Samejima, T. *J. Biochem. (Tokyo)* **1999**, *125*, 662−668.
(28) Hall, J. F.; Kanbi, L. D.; Strange, R. W.; Hasnain, S. S. *Biochemistry* **1999**, *38*, 12675−12680.
(29) Diederix, R. E. M.; Canters, G. W.; Dennison, C. *Biochemistry* **2000**, *39*, 9551−9560.
(30) Hough, M. A.; Hall, J. F.; Kanbi, L. D.; Hasnain, S. S. *Acta Crystallogr., Sect. D: Biol. Crystallogr.* **2001**, *D57*, 355−360.
(31) Veselov, A.; Olesen, K.; Sienkiewicz, A.; Shapleigh, J. P.; Scholes, C. P. *Biochemistry* **1998**, *37*, 6095−6105.
(32) Bonander, N.; Karlsson, B. G.; Vänngård, T. *Biochemistry* **1996**, *35*, 2429−2436.
(33) Murphy, L. M.; Strange, R. W.; Karlsson, B. G.; Lundberg, L. G.; Pascher, T.; Reinhammar, B.; Hasnain, S. S. *Biochemistry* **1993**, *32*, 1965−1975.
(34) Vidakovic, M.; Germanas, J. P. *Angew. Chem., Int. Ed. Engl.* **1995**, *34*, 1622−1624.
(35) Tsai, L.-c.; Bonander, N.; Harata, K.; Karlsson, G.; Vänngård, T.; Langer, V.; Sjölin, L. *Acta Crystallogr., Sect. D: Biol. Crystallogr.* **1996**, *D52*, 950−958.
(36) Farver, O.; Skov, L. K.; Pascher, T.; Karlsson, B. G.; Nordling, M.; Lundberg, L. G.; Vänngård, T.; Pecht, I. *Biochemistry* **1993**, *32*, 7317−7322.
(37) Bauer, R.; Danielsen, E.; Hemmingsen, L.; Bjerrum, M. J.; Hansson, O.; Singh, K. *J. Am. Chem. Soc.* **1997**, *119*, 157−162.
(38) Salgado, J.; Kroes, S. J.; Berg, A.; Moratal, J. M.; G. W., C. *J. Biol. Chem.* **1998**, *273*, 177−185.
(39) Frank, P.; Licht, A.; Tullius, T. D.; Hodgson, K. O.; Pecht, I. *J. Biol. Chem.* **1985**, *260*, 5518−5525.
(40) Solomon, E. I.; Penfield, K. W.; Gewirth, A. A.; Lowery, M. D.; Shadle, S. E.; Guckert, J. A.; LaCroix, L. B. *Inorg. Chim. Acta* **1996**, *243*, 67−78.
(41) Palmer, A. E.; Randall, D. W.; Xu, F.; Solomon, E. I. *J. Am. Chem. Soc.* **1999**, *121*, 7138−7149.
(42) DeBeer, S.; Randall, D. W.; Nersissian, A. M.; Valentine, J. S.; Hedman, B.; Hodgson, K. O.; Solomon, E. I. *J. Phys. Chem. B* **2000**, *104*, 10814−10819.
(43) Randall, D. W.; George, S. D.; Holland, P. L.; Hedman, B.; Hodgson, K. O.; Tolman, W. B.; Solomon, E. I. *J. Am. Chem. Soc.* **2000**, *122*, 11632−11648.
(44) Lu, Y.; LaCroix, L. B.; Lowery, M. D.; Solomon, E. I.; Bender, C. J.; Peisach, J.; Roe, J. A.; Gralla, E. B.; Valentine, J. S. *J. Am. Chem. Soc.* **1993**, *115*, 5907−5918.
(45) Han, J.; Loehr, T. M.; Lu, Y.; Valentine, J. S.; Averill, B. A.; Sanders-Loehr, J. *J. Am. Chem. Soc.* **1993**, *115*, 4256−4263.
(46) LaCroix, L. B.; Shadle, S. E.; Wang, Y.; Averill, B. A.; Hedman, B.; Hodgson, K. O.; Solomon, E. I. *J. Am. Chem. Soc.* **1996**, *118*, 7755−7768.
(47) Messerschmidt, A.; Prade, L.; Kroes, S. J.; Sanders-Loehr, J.; Huber, R.; Canters, G. W. *Proc. Natl. Acad. Sci. U.S.A.* **1998**, *95*, 3443−3448.
(48) LaCroix, L. B.; Randall, D. W.; Nersissian, A. M.; Hoitink, C. W. G.; Canters, G. W.; Valentine, J. S.; Solomon, E. I. *J. Am. Chem. Soc.* **1998**, *120*, 9621−9631.
(49) Andrew, C. R.; Yeom, H.; Valentine, J. S.; Karlsson, B. G.; van Pouderoyen, G.; Canters, G. W.; Loehr, T. M.; Sanders-Loehr, J.; Bonander, N. *J. Am. Chem. Soc.* **1994**, *116*, 11489−11498.
(50) Randall, D. W.; Gamelin, D. R.; LaCroix, L. B.; Solomon, E. I. *J. Biol. Inorg. Chem.* **2000**, *5*, 16−29.
(51) Donaire, A.; Jimenez, B.; Fernandez, C. O.; Pierattelli, R.; Niizeki, T.; Moratal, J.-M.; Hall, J. F.; Kohzuma, T.; Hasnain, S. S.; Vila, A. J. *J. Am. Chem. Soc.* **2002**, *124*, 13698−13708.
(52) Fernandez, C. O.; Niizeki, T.; Kohzuma, T.; Vila, A. J. *J. Biol. Inorg. Chem.* **2003**, *8*, 75−82.
(53) Olsson, M. H. M.; Ryde, U. *J. Biol. Inorg. Chem.* **1999**, *4*, 654−663.
(54) Donaire, A.; Jimenez, B.; Moratal, J.-M.; Hall, J. F.; Hasnain, S. S. *Biochemistry* **2001**, *40*, 837−846.
(55) Machczynski, M. C.; Gray, H. B.; Richards, J. H. *J. Inorg. Biochem.* **2002**, *88*, 375−380.

~30 mV (from 308 to 333 mV). We wish to expand upon this work by investigating ways for specific replacement of the axial methionine with selenomethionine because the Met auxotroph approach replaces all six methionine residues in azurin with selenomethionines. This makes it difficult in certain studies (such as XAS) to focus on the specific axial selenomethionine. It is also desirable to design methods for 100% replacement of Met with SeMet, as the incorporation efficiency of SeMet using the Met auxotroph was up to 85%,[39] making it possible for Met-containing proteins to interfere in the study of SeMet proteins. Finally, we wish to replace Met with other amino acids, such as Nle as well.

There are a number of methods for incorporating unnatural amino acids into proteins.[56−59] The development of the expressed protein ligation (EPL) method enabled coupling of a bacterially expressed peptide to a synthetic peptide without protecting groups, thus allowing facile incorporation of unnatural amino acids in enough quantities for spectroscopic and X-ray crystallographic studies.[60,61] The only requirement is a cysteine residue at the joint of the expressed protein and the synthetic peptide containing the unnatural amino acid.

Azurin is an ideal choice for the application of EPL. Blue copper azurin is 128 amino acids long. The copper coordinating residues Cys112, His117, and Met121 are located in the final 17 amino acids. Furthermore, the Cys112 residue is at an ideal location for coupling the expressed recombinant protein, containing the first 111 amino acids, with the C-terminal peptide, containing the desired unnatural amino acids. In addition, azurin is highly stable, as exemplified by the expression, purification, and characterization of the mutant with its C-terminal peptide deleted from Met121.[19] In azurin, Met121 can be systematically mutated by coupling the same 111 amino acid N-terminal fragment to different synthetic C-terminal peptides by EPL.

In this paper, a series of unnatural amino acid mutations was designed to systematically probe the role of the axial methionine ligand. Unnatural mutant proteins where Met121 was replaced by norleucine and selenomethionine were constructed. An increase in axial ligand interaction was hypothesized, at least for the Cu(I) state, with an axial selenomethionine, while the presence of norleucine was intended to cause a decrease in ligand interaction, with minimal steric perturbations. For additional comparison, the natural amino acid mutant Met121Leu was also prepared. UV−visible absorption spectra, multifrequency EPR spectra, reduction potentials, and Cu and Se EXAFS data of the variants are presented. A careful analysis, including the plot of observed reduction potentials of the WT azurin and its variants obtained in this work and the corresponding hydrophobicity of the axial ligand side chain defined by the log of the partition coefficient (log *P*), revealed hydrophobicity as the dominant factor in tuning the reduction potentials of blue copper centers by axial ligands. The results are discussed in the context of the role of this residue.

Experimental Section

All chemicals utilized were of analytical grade or higher. The gene fragment corresponding to the first 111 amino acids of *Pseudomonas aeruginosa* azurin was cut out of the WT azurin pet9a plasmid, obtained as a generous gift from Professor John H. Richards. The fragment was ligated into the commercially available pTXB1 vector (New England Biolabs, Beverly, MA),[62] and the azurin-intein-chitin binding domain fusion protein was expressed at 30 °C in BLR(DE3) E. coli (Novagen, Madison, WI) grown in 2 L of LB medium. Collected cells were lysed with a French pressure cell in 20 mM TrisHCl pH 8.0, 500 mM NaCl, 1 mM EDTA, 1 mM PMSF, 0.1% Triton X-100. Inclusion bodies were denatured with a final concentration of 4 M urea. After centrifugation, the supernatant was diluted with buffer (20 mM TrisHCl pH 8.0, 500 mM NaCl) to a final concentration of 2 M urea, divided into three fractions, and passed down 3 × 8.5 mL chitin bead columns. The beads were washed with 5 column volumes of fresh urea buffer (20 mM TrisHCl pH 8.0, 500 mM NaCl, 2 M urea), followed by 2 column volumes of buffer without urea. The cleavage buffer (20 mM TrisHCl pH 8, 500 mM NaCl, 1 mM EDTA, and 50 mM 2-mercaptoethanesulfonic acid (MESNA)) was then added to the columns with 5−10 mg of the synthetic peptide (~1 mM). Reactions were allowed to proceed on the chitin column for 40−60 h at 4 °C. After the reaction, the proteins were eluted from the column and exchanged into 50 mM NH_4OAc pH 5.1 for study. The reactions yielded 2−4 mg of product per 8.5 mL of chitin beads (1 L of cell culture), corresponding to 33−67% yield. If necessary, the proteins were purified on a POROS 20 HQ anion-exchange resin with a BioCad Sprint HPLC system (PerSeptive Biosystems, Farmingham, MA). The synthetic peptide sequences (H_2N-CysThrProGlyHisSerAlaLeu(Met or Nle or SeM)-LysGlyThrLeuThrLeuLys-COOH) were synthesized using highly optimized Boc-solid-phase peptide synthesis protocols on Boc-Lys-OCH_2-PAM resin. Following chain assembly, peptides were cleaved from their solid supports by treatment with anhydrous HF. Crude peptides were purified by preparative reverse-phase HPLC and analyzed by electrospray mass spectrometry. The Met121Leu azurin variant was synthesized using Quikchange mutagenesis techniques (Stratagene, La Jolla, CA), expressed, and isolated analogous to previous protocols.[63,64]

UV−visible absorption spectra were collected at ambient temperature on a Varian CARY 3E spectrophotometer. X-band EPR spectra were collected on a Varian E-122 spectrometer. The samples were run as frozen glasses at ~50 K using liquid He and an Air Products Helitran cryostat. Q-band EPR spectra were collected on a Bruker 300 Elexsys system with a Q-band ER5106T TE011 cavity. Samples were run frozen at ~50 K with liquid He using an Oxford CF935 Cryostat and an Oxford ITC-4 temperature controller. The magnetic fields were calibrated with a Varian NMR Gauss meter. All instruments were maintained by the University of Illinois NIH EPR Research Center. The reduction potentials were obtained using a pyrolytic graphite edge (PGE) electrode (assembled as described in ref 65) in 20 mM NaOAc pH 4.0. The protein was adsorbed on the graphite edge surface by soaking overnight at 4 °C. Cyclic voltammetry scans were run in 20 mM NaOAc pH 4.0, 2 M NaCl solution, incubated on ice. The potentiostat was a CH Instruments model 620A Electrochemical Analyzer. Reduction potentials and peak separations behaved as described by Armstrong et al.[65]

The log of the partition coefficient (log *P*) was used to quantify the hydrophobicity of the amino acid side chains. The values for the side chain only of Nle, Leu, SeM, and Met were calculated according to

(56) Merrifield, B. *Methods Enzymol.* **1997**, *289*, 3−13.
(57) Dawson, P. E.; Muir, T. W.; Clark-Lewis, I.; Kent, S. B. H. *Science* **1994**, *266*, 776−779.
(58) Low, D. W.; Hill, M. G. *J. Am. Chem. Soc.* **1998**, *120*, 11536−11537.
(59) Low, D. W.; Hill, M. G. *J. Am. Chem. Soc.* **2000**, *122*, 11039−11040.
(60) Muir, T. W.; Sondhi, D.; Cole, P. A. *Proc. Natl. Acad. Sci. U.S.A.* **1998**, *95*, 6705−6710.
(61) Severinov, K.; Muir, T. W. *J. Biol. Chem.* **1998**, *273*, 16205−16209.
(62) Evans, T. C., Jr.; Benner, J.; Xu, M.-Q. *Protein Sci.* **1998**, *7*, 2256−2264.
(63) Hay, M.; Richards, J. H.; Lu, Y. *Proc. Natl. Acad. Sci. U.S.A.* **1996**, *93*, 461−464.
(64) Hay, M. T.; Ang, M. C.; Gamelin, D. R.; Solomon, E. I.; Antholine, W. E.; Ralle, M.; Blackburn, N. J.; Massey, P. D.; Wang, X.; Kwon, A. H.; Lu, Y. *Inorg. Chem.* **1998**, *37*, 191−198.
(65) Jeuken, L. J. C.; Armstrong, F. A. *J. Phys. Chem. B* **2001**, *105*, 5271−5282.

the method of Leo et al.[66] A fragment constant of −0.59 was used for the selenoether group.[67]

XAS data were collected at the Stanford Synchrotron Radiation Laboratory (SSRL) on beam lines 7.3 (BL 7.3) and 9.3 (BL 9.3) operating at 3.0 GeV with beam currents between 100 and 50 mA. Si220 monochromators with 1.2-mm slits were used to provide monochromatic radiation in the 8.8−9.7 (Cu K-edge) and 12.4−13.4 (Se K-edge) keV energy range. Harmonic rejection was achieved either by detuning the monochromator 50% at the end of the scan (BL 7.3, Cu and Se edges) or by means of a rhodium-coated mirror with a cutoff of 13 keV placed upstream of the monochromator (BL 9.3, Cu edges). The protein samples were measured as frozen glasses in 20−30% ethylene glycol at 11−14 K in fluorescence mode using either a 13-element (BL 7.3) or a 30-element (BL 9.3) Canberra Ge detector. On BL 7.3, the count rate of each detector channel was kept below 110 kHz, while the rise in fluorescent counts through the edge was kept below 20 kHz per channel. Count rates were linear over this range, and no dead-time correction was necessary. For measurement of Cu XAS on BL 9.3, a Soller slit assembly fitted with a 6 μ Ni filter was used in conjunction with the 30-element detector to decrease the elastic scatter peak, and protect against detector saturation. Here, maximum count rates per channel did not exceed 40 kHz. The summed data for each detector channel were then inspected, and only those channels that gave high-quality backgrounds free from glitches, drop outs, or scatter peaks were included in the final average. Data reduction was performed as follows. First, a blank data file collected under identical conditions and detector geometry was subtracted from the summed experimental data. This procedure removed any residual K_β fluorescence from the Ni filter which was still present in the detector window, and produced a flat preedge close to zero. Background subtraction was carried out using the PROCESS module of EXAFSPAK[68] using a Gaussian fit to the preedge region, and a cubic spline fit with k^4 weighting in the postedge region. The E_0 (start of the EXAFS) was chosen as 9000 eV for Cu and 12 675 eV for Se. The EXAFS data were k^3-weighted, and Fourier transformed over the range $k = 0-12.8$ Å^{-1} (Cu) or $k = 0-14$ Å^{-1} (Se). Sequential scans were examined for evidence of radiation damage and/or photoreduction. For oxidized samples, photoreduction was observed to occur after the first or second scan of a series, as evidenced from a small shift in the energy of the calibrated absorption edge. For these samples, only the first scan of the series was used in the EXAFS analysis. In all cases, the signal-to-noise ratio of the first scan was good enough to provide accurate distances.

Data analysis was performed using the OPT module of the EXAFSPAK computer suite.[68] Theoretical phase and amplitude functions were calculated using FEFF 8.0.[69] The EXAFS data were simulated using a nonlinear Marquadt algorithm where the difference between experimental and the calculated data is minimized. For Cu edge data, coordination numbers were fixed at the crystallographically determined values for equatorial ligands, that is, 2 N from histidine and 1 S from cysteine. Contributions from axial ligands (for example, Se in the M121Semet derivative) were tested as to the importance of their contribution to the total EXAFS, again using the crystal structure of the WT enzyme as a starting model. For Se edges of the SeMet derivatives, the coordination number of the first shell C atoms was fixed at 2, and contribution from the expected Se−Cu interaction was added as required. Variable parameters refined in the fit were as follows: ΔE_0 (a small energy correction at $k = 0$, ranging depending on the oxidation state of the metal), Ri (the distance between the central absorber and atom i), and σ^2 (the Debye−Waller factor, defining the mean square deviation of Ri). EXAFS fits from derivatives of the same oxidation state and similar ligation are expected to exhibit very similar values of ΔE_0. When E_0 was allowed to float freely, small variations in E_0 were observed (±1.5 eV for oxidized samples, and ±3 eV for reduced samples). Because R and ΔE_0 are correlated, variability in E_0 can lead to lower precision in the determination of distances. Consequently, for distance comparisons between the derivatives of the same oxidation state, metrical parameters were refined using a fixed average value of ΔE_0. Multiple (double and triple) scattering pathways between the Cu absorber and the outer-shell C scatterers of the imidazole ligands were calculated using FEFF and included if they exceeded 20% of the Cu−N(imidazole) single scattering intensity. A goodness-of-fit (F_w) parameter, displayed at the end of each cycle, was used to determine the merit of the fit. F_w is defined as follows:

$$F_w = \sum_{i=1}^{n} \frac{k^6(\text{data} - \text{model})^2}{k^6(\text{data})^2}$$

Table 1. Mass Spectrometry Results for the EPL Proteins

	apo (Da)	holo (Da)
EPL WT azurin		
calc.:	13945.8	14008.4
exptl.:	13945 ± 6.9	14005 ± 7.0
M121Nle azurin		
calc.:	13927.8	13990.4
exptl.:	13924 ± 6.9	13984.8 ± 7.0
M121SeM azurin		
calc.:	13992.7	14055.2
exptl.:	13989.8 ± 7.0	14052.8 ± 7.1

Results

To first demonstrate that EPL could be used to synthesize authentic and properly folded wild-type azurin, we coupled the 17 amino acid, C-terminal synthetic peptide corresponding to the *P. aeruginosa* WT azurin sequence to the bacterially expressed 111 amino acid N-terminal segment. The coupling of the synthetic fragment to the expressed fragment was confirmed by electrospray mass spectrometry for both the apo- and the holo-proteins (Table 1). The UV−visible absorption and X-band EPR spectra of the EPL azurin were found to be identical to those of the recombinant *P. aeruginosa* WT azurin (Figure 2),[19−25] indicating that azurin made by the EPL method has the same overall and active site structure as WT azurin made by standard methods.

Variants in which Met121 was replaced with norleucine and selenomethionine were obtained by EPL coupling to the corresponding C-terminal peptides. Mass spectroscopic analysis confirmed correct assembly of both the apo- and the holo-proteins (Table 1). The variants display similar intense visible absorption around 630 nm, assignable to a S(Cys) to Cu(II) charge transfer (CT) transition (Figure 3).[7,14,70] As compared to WT azurin, the CT band red-shifts ∼4 nm in the Nle and SeM variants, and ∼5 nm in the Leu variant (Figure 3 and Table 2). The X- and Q-band EPR spectra of the variants are also very similar to those of WT azurin (Figure 4). Simulation of the both the X- and the Q-band EPR spectra[71,72] yields more accurate g and A values for the variants (Table 2). The $A_\parallel$ values of the variants are smaller than WT (63 G), with the SeM variant

(66) Abraham, D. J.; Leo, A. J. *Proteins: Struct., Funct., Genet.* **1987**, *2*, 130−152.
(67) Leo, A. J., personal communication.
(68) George, G. N. Stanford Synchrotron Radiation Laboratory, Menlo Park, CA, 1995.
(69) Ankudinov, A. L.; Ravel, B.; Rehr, J. J.; Conradson, S. D. *Phys. Rev. B: Condens. Matter* **1998**, *58*, 7565−7576.
(70) Gewirth, A. A.; Solomon, E. I. *J. Am. Chem. Soc.* **1988**, *110*, 3811−3819.
(71) Nilges, M. J. SIMPIPM EPR simulation program obtained from the Illinois EPR Research Center (IERC), University of Illinois.
(72) Nilges, M. J. Ph.D. Thesis, University of Illinois, 1979.

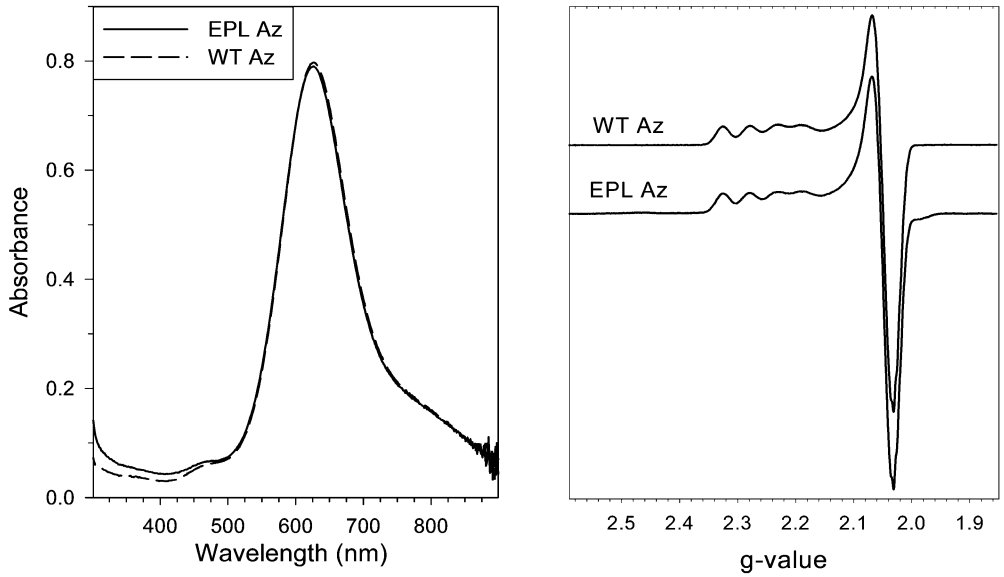

Figure 2. UV−visible absorption (left) and X-band EPR spectra (right) of WT and EPL azurin.

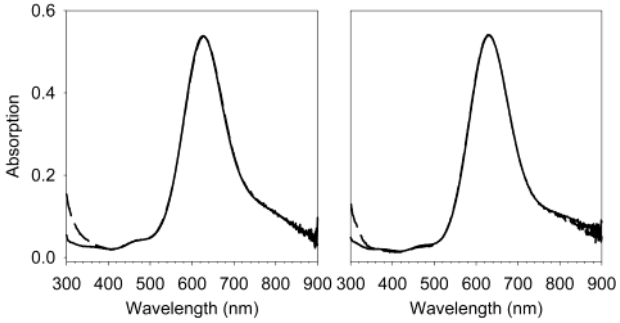

Figure 3. UV−visible absorption of the azurin variants (left, solid = WT, dashed = M121SeM) (right, solid = M121Leu, dashed = M121Nle).

Table 2. Tabulated Spectroscopic Data and Reduction Potentials for the M121X Mutant Series

	abs peaks, nm	EPR *g* (A)	E_0 (mV vs NHE)
WT azurin		$g_1 = 2.2620$ (63.5 G)	
	626	$g_2 = 2.0568$ (12.7 G)	315
		$g_3 = 2.0388$ (12.7 G)	
M121Nle azurin		$g_1 = 2.2680$ (58.8 G)	
	630	$g_2 = 2.0584$ (19.6 G)	455
		$g_3 = 2.0402$ (13.4 G)	
M121Leu azurin		$g_1 = 2.2706$ (57.0 G)	
	631	$g_2 = 2.0578$ (19.2 G)	450
		$g_3 = 2.0395$ (13.2 G)	
M121SeM azurin		$g_1 = 2.2585$ (60.6 G)	340
	629	$g_2 = 2.0565$ (12.1 G)	340
		$g_3 = 2.0386$ (13.2 G)	

(61 G) being the closest to the WT, the Leu derivative (57 G) being furthest from the WT, and the Nle variant (59 G) being in between. The red-shifted CT band and the smaller $A_{||}$ are consistent with a more covalent S(Cys)−Cu bond in those variants.

The reduction potentials were obtained using a pyrolytic graphite edge (PGE) electrode[65] in 20 mM NaOAc pH 4.0. The cyclic voltammogram for the WT protein film (Figure 5) yielded a potential of 315 mV versus the normal hydrogen electrode (NHE). This result is in good agreement with those published previously with PGE electrodes[65] and close to the measured values of 304−314 mV in other studies.[73,74] The potentials of the M121Nle (455 mV vs NHE) and M121Leu (450 mV vs NHE) variants were around 140 mV higher than the WT values, while the M121SeM variant's potential (340 mV vs NHE) was around 25 mV higher, all consistent with previously published data with Leu and SeM.[19,22,39] The voltammetry data indicate that altering the nature of the axial ligand significantly alters the reduction potential of the site.

Cu-edge X-ray absorption fine structure (EXAFS) data were collected on the oxidized WT, M121SeM, and M121Nle proteins and the reduced M121SeM, M121Nle, and Met121Leu proteins. The results from the data fits are given in Table 3, and best fits for oxidized WT, and oxidized and reduced M121SeM, are compared in Figure 6a−c. Generally, the data indicate that mutating the methionine residue in azurin to Leu, Nle, or SeM has little effect on the overall structure of the metal-binding site. The EXAFS of the oxidized WT azurin gives parameters in good agreement with results obtained previously,[33,42,75] two histidines coordinated at 1.92 ± 0.01 Å, with a short Cu−S interaction at 2.14 ± 0.01 Å. The data show no sign of any contribution from the S of the methionine ligand, again consistent with previous observations. Data for the reduced form of WT azurin are included for comparison to the variants.[76] These data demonstrate that the blue copper center of the WT azurin produced by the semisynthetic EPL route is isostructural with azurin isolated by conventional methods, at least with respect to metrical parameters.

The only significant difference between the M121Nle variant and WT azurin is a 0.05 Å lengthening of the Cu−S(Cys) bond length. The Nle substitution thus appears to slightly weaken the copper−cysteine bond. XAS gives no evidence as to whether this is a steric or electronic effect.

The M121SeM oxidized derivative behaves very similarly to the Nle derivative, in that the Cu−S(Cys) bond is lengthened

(73) Goldberg, M.; Pecht, I. *Biochemistry* **1976**, *15*, 4197−4208.
(74) Van Pouderoyen, G.; Mazumdar, S.; Hunt, N. I.; Hill, H. A. O.; Canters, G. W. *Eur. J. Biochem.* **1994**, *222*, 583−588.
(75) Canters, G. W.; Kolczak, U.; Armstrong, F.; Jeuken, L. J. C.; Camba, R.; Sola, M. *Faraday Discuss.* **2000**, *116*, 205−220.
(76) DeBeer, S.; Wittung-Stafshede, P.; Leckner, J.; Karlsson, G.; Winkler, J. R.; Gray, H. B.; Malmström, B. G.; Solomon, E. I.; Hedman, B.; Hodgson, K. O. *Inorg. Chim. Acta* **2000**, *297*, 278−282.

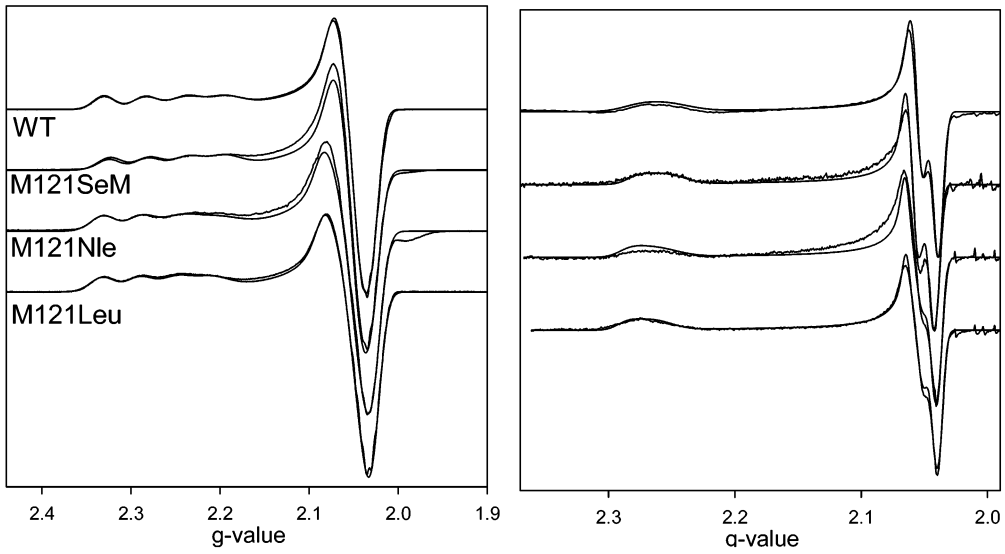

Figure 4. X-band (left) and Q-band (right) EPR spectra of the azurin variants. Simulations are the thin, smooth lines, and experimental data are the noisy lines.

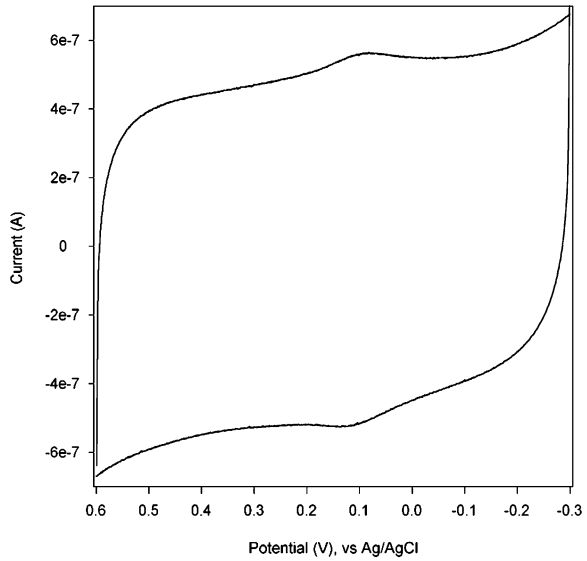

Figure 5. Cyclic voltammogram of WT azurin − modified graphite edge electrode versus Ag/AgCl. Conditions: 500 mV/s scan rate, 10 s quiet time at oxidizing end, in 20 mM NaOAc pH 4.0 and 2.0 M NaCl, 0 °C.

to 2.18 Å. It is interesting to note the presence of the heavy selenium atom in the oxidized form of the M121SeM mutant does not result in an observable backscattering contribution from the axial position. This is likely due to the predicted long (>3 Å) separation between the copper ion and selenium ligand. This derivative also allows the copper selenomethionine interaction to be probed by Se K edge measurements (Figure 6d). The Se K EXAFS can be simulated (as expected) by 2 C at 1.95 Å. The spectrum is dominated by the first shell and shows no contribution from Se−Cu, although some more distant outer-shell scattering can be seen in the FT. Including outer-shell Se−Cu and Se−S interactions in the fits gave no improvement in F_w. These data emphasize that the copper−methionine interaction is extremely weak. The similarity in active site structures between WT and the variants is not surprising given the known rigidity of the azurin active site, recently attributed to the outer-sphere hydrogen-bonding network surrounding the active site.[55]

Table 3. Parameters Used To Simulate the Cu K Edge and Se K Edge EXAFS of Derivatives of Azurin Synthesized by Expressed Protein Ligation[a]

	oxidized form[b]					reduced form				
	N	*R*/Å	DW/Å^2	Fw	ΔE_0/eV	N	*R*/Å	DW/Å^2	Fw	ΔE_0/eV
WT Azurin										
Cu K edge EXAFS	2 N 1 S	1.92 2.14	0.003 0.004	0.38	−9.82	2 N 1 S	2.00 2.21	0.003 0.003	0.41[c]	
M121Nle Azurin										
Cu K edge EXAFS	2 N 1 S	1.95 2.19	0.004 0.003	0.34	−9.82	2 N 1 S	2.02 2.24	0.004 0.002	0.20	−6.50
M121SeM Azurin										
Cu K edge EXAFS	2 N 1 S	1.95 2.18	0.004 0.006	0.37	−9.82	2 N 1 S	2.02 2.26	0.002 0.007	0.20	−6.50
Se K edge EXAFS	2C	1.95	0.002	0.42	−5.57					
M121Leu Azurin										
Cu K edge EXAFS						2 N 1 S	2.01 2.23	0.005 0.004	0.25	−6.50

[a] Multiple scattering contributions from outer-shell atoms of imidazole rings were simulated using FEFF 8.0. First shell distances are accurate to ±0.01 Å. Coordination numbers were set at values expected from azurin crystal structures. [b] Metrical parameters at the Cu edges were determined by simulation of the first scan only due to evidence of a small amount of photoreduction in the second and subsequent scans. [c] From *Inorg. Chim. Acta* **2000**, *297*, 278.

The EXAFS of the reduced derivatives shows the expected lengthening of both the Cu−N(His) and the Cu−S(Cys) bonds documented previously for WT azurin (Table 3).[76] For example, the Cu−S(Cys) bond lengths in WT, M121Nle, and M121SeM increase by 0.07, 0.05, and 0.08 Å, respectively, with comparable increases in the Cu−N(His) distances.

Discussion

Site-directed mutagenesis has been used extensively to probe the role of specific residues in protein structure and function. The limitation of only natural amino acids for this method often makes it difficult to separate multiple factors involved in the site-directed mutagenesis. Therefore, it is desirable to replace the residues in question with unnatural amino acids at a reasonable cost and with enough yields for spectroscopic and X-ray crystallographic studies. Furthermore, introducing unnatural amino acids into metalloproteins may allow design and

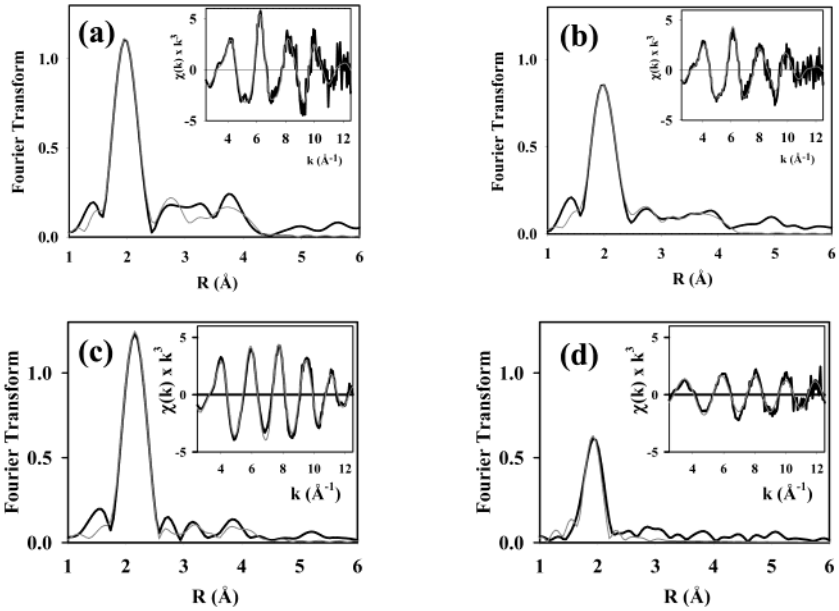

Figure 6. Fourier transforms and EXAFS (insets) for WT azurin and the selenomethionine variant produced by EPL. Experimental data are represented by thick lines; simulated data are represented by thin lines. (a) WT, (b) oxidized SeM, Cu edge, (c) reduced SeM, Cu edge, (d) oxidized SeM, Se edge. FTs are phase corrected, transformed over the range $k = 0-12.8$ Å^{-1}, copper edge, or $k = 0-14$ Å^{-1}, Se edge.

engineering of new artificial metalloproteins with tunable structural and functional properties.[77] The recently developed EPL method[60,61] can accomplish this goal.

To demonstrate and explore the utility of this method in elucidating the role of amino acids in protein metal-binding sites, we replace Met121, an axial ligand in blue copper azurin, with selenomethionine and norleucine using the EPL method. To our knowledge, this study is the first time an unnatural amino acid has been introduced into the active site of a metalloprotein using EPL (we have communicated a successful replacement of active site Cys112 with selenocysteine, the 21st amino acid[78]). The yield obtained here (5 mg/L of media) is typical of EPL experiments, and the protein variants obtained allowed us to carry out all routine spectroscopic and crystallographic studies. Because mass spectrometry, UV−vis, EPR, and XAS spectra of the WT azurin obtained by EPL are identical to those of WT azurin obtained by standard methods, the EPL method can be used to introduce unnatural amino acids into metalloproteins. The unnatural amino acids were chosen for this study on the basis of structural and steric similarity to the native methionine. However, despite the structural similarity, the methylene group in the Nle variant introduces two protons that may have some steric differences as compared to Met.

Results shown in Figures 3 and 4 and summarized in Table 2 indicate that all Met121 mutations resulted in red-shifts of the S(Cys)-to-Cu(II) CT band around 625 nm, and smaller hyperfine coupling constants in the parallel region of EPR. There is a 4 nm red-shift in the S(Cys)-to-Cu(II) CT band in going from WT(Met121) to Met121SeMet and Met121Nle azurins, and a further, 5 nm red-shift for the Met121Leu variant. There are also similar differences between the EPR parameters. For example, the $A_{||}$ of Met121SeMet azurin (60.6 G) is closest to that of WT azurin (63.5 G), while $A_{||}$ of Met121Leu azurin (57.0 G) deviates furthest from that of WT azurin. The red-shift of the CT band and the narrowing of the $A_{||}$ suggest a more covalent S(Cys)−Cu(II) bond in the variants. The small shifts in energy of the CT band and $A_{||}$ values have been observed in other Met121 mutations[19−25] and are consistent with the fact that Met121, being in an axial position and ∼3.0 Å away from the copper center, exerts only a weak influence on the Cu(II) state of the center.

In contrast to the small spectral changes associated with the mutations, large increases in reduction potentials were observed. Replacing Met121 with SeM, Leu, and Nle resulted in a reduction potential increase of ∼25, 135, and 140 mV, respectively. Several factors have been proposed to contribute to the reduction potentials of blue copper proteins.[5,6,75] They include metal−ligand interactions in the equatorial plane and in the axial positions, geometry of the metal center, hydrophobicity around the metal center, the environment at the secondary coordination sphere (such as hydrogen-bonding patterns), and solvent exposure of the site. In this paper, we are concerned with the axial ligand interaction. When one mutation is made at the metal-binding site, such as at the axial Met121, many and maybe all of the above factors may be changed. It has been difficult to quantify each of the contributions. For example, the high reduction potential of Met121Leu azurin has been observed before. Because Met121 is replaced with sterically different Leu, it is difficult to define or quantify changes this mutation brings because introduced steric conflict in the Met121Leu mutant may, for example, change the solvent exposure and disrupt the secondary coordination sphere of the center. The work presented here makes it possible to deconvolute several of these factors. Because the structural difference between Nle121 and Leu121 causes only small, ∼5 mV, reduction potential changes, we can conclude that factors due to the subtle steric differences of Leu and Nle play only a minor role in determining the reduction potentials of the blue copper center. Instead, because both Met121Leu and Met121Nle mutations resulted in similar large, ∼140 mV increases in reduction potentials, factors common to

(77) Lu, Y.; Berry, S. M.; Pfister, T. D. *Chem. Rev.* **2001**, *101*, 3047−3080.
(78) Berry, S. M.; Gieselman, M. D.; Nilges, M. J.; Van der Donk, W. A.; Lu, Y. *J. Am. Chem. Soc.* **2002**, *124*, 2084−2085.

those two residues, such as changes in axial ligand interaction and hydrophobicity, must be important.

On the basis of the above analysis, we therefore can attribute the dramatic increases in reduction potentials in the Met121 variants to changes in axial ligation, hydrophobicity, or solvent accessibility. A recent study has shown that the reduction potential of unfolded azurin is higher than that of the folded azurin.[79,80] The authors attributed the downshift of the potential in the folded state to the rack-induced axial coordination that stabilizes Cu(II) relative to Cu(I). Replacement of Met121 to noncoordinating Leu and Nle would abolish this axial interaction in a fashion similar to protein unfolding, causing the stabilization of the Cu(I) state and an increase in the potential.[5,6,22] In support of this interpretation, the potentials of Met121Leu (450 mV) and Met121Nle (455 mV) azurin are strikingly similar to that of denatured WT azurin (456 mV).[79,80] The hydrophobic effect of Met121Leu and Met121Nle mutations makes additional contributions to the large increase in reduction potentials by destabilizing the highly charged Cu(II) state. In the case of the M121SeM variant, the increase in potential could arise from a further stabilization of the Cu(I) state by the Se donor. It is interesting to note that axial ligand variations in Cu_A centers influence these properties to a lesser extent.[81,82]

X-ray absorption spectroscopy has also been used to examine the structural environment of the active site copper in the azurin variants produced by EPL. The metrical parameters observed for the oxidized WT derivative are in excellent agreement with those published previously, establishing that the EPL protocol faithfully reproduces the cupredoxin active site structure. However, the EXAFS analysis of the variant proteins reveals structural trends which are not entirely consistent with the conclusion that axial ligation is the primary influence on redox potential. First, all variants show a lengthening of the Cu−S bond with respect to WT, which is most pronounced in the Nle variant. The increase in Cu−S bond length would normally imply a decrease in bond strength, that is, the opposite effect to that inferred from analysis of visible and EPR spectroscopic data which were suggestive of an increase in Cu−S covalency. Our data are consistent with findings by Vila and co-workers, who showed that, in certain blue copper proteins such as pseudoazurin and rusticyanin, the copper−axial ligand interaction does not necessarily affect the Cu−S bond strength.[51,52] Instead, other factors from the environment around the copper center play more important roles.

The second trend, revealed by EXAFS analysis of the M121SeM variant, is the weakness of the methionine interaction, and by inference the relative unimportance of the axial interaction in stabilizing the site. Substitution of a single methionine by selenomethionine at residue 112 has allowed the Cu−Se interaction to be probed by both Cu and Se XAS. In neither case can a Cu−Se interaction be detected. This contrasts with the situation observed for the M160SeM derivative of *T. thermophilus* cytochrome ba_3 soluble subunit II where the methionine is a ligand to the dinuclear Cu_A center.[81] Here, strong Se−Cu scattering is observed with a Se−Cu bond length of 2.55 Å in both oxidized and reduced proteins. In contrast to azurin, the M160SeM variant of Cu_A has no effect on the redox potential. This poses the question as to why the stronger 2.55 Å Cu−SeM interaction would lead to no stabilization of the Cu(I) state in Cu_A when the much weaker and undetectable Cu−SeM interaction in azurin leads to a 25 mV increase in potential suggestive of Cu(I) stabilization.

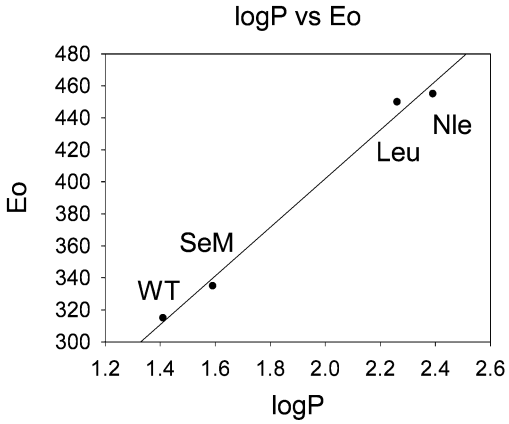

Figure 7. Plot of log *P* for the amino acid side chain versus the reduction potential of the M121 azurin variant.

These observations may suggest that, in the azurin case, the observed changes in redox potential of M121SeM originate from other factors, such as hydrophobicity. To support this conclusion, we examined the relationship between the observed reduction potentials of the WT azurin and its variants obtained in this work and the corresponding hydrophobicity of the axial ligand side chain defined by the log of the partition coefficient (log *P*). The values of log *P* were calculated according to the method of Leo et al.[66] for the side chain of each variant amino acid. A linear correlation was obtained with an r^2 factor of 0.9915 (Figure 7). This result, together with observations described above, strongly suggests that hydrophobicity is the most dominant factor in the axial ligand's role of determining the reduction potential of the blue copper center.

In conclusion, we have shown that the expressed protein ligation method can be used to introduce unnatural amino acids into the metal-binding site of proteins at costs and yields suitable for biochemical and biophysical studies. The isostructural replacement of Met121 with SeMet and Nle allowed us to deconvolute factors influencing the reduction potentials of the blue copper azurin by this axial ligand and pointed to hydrophobicity as the dominate factor. Further application of the EPL method to this and other metalloproteins will make it possible to not only probe roles of different residues more accurately, but also design new metalloproteins with tunable structural and functional properties.

Acknowledgment. This research was supported by the National Science Foundation (CHE-0139203 to Y.L.) and National Institutes of Health (GM54803 to N.J.B.). We thank Prof. Michael G. Hill at Occidental College, and Prof. Fraser Armstrong and Dr. Kevin Hoke of Oxford University for helpful suggestions on electrochemistry, Prof. Andrew Gewirth for the kind gift of pyrolytic graphite, Prof. Wilfred van der Donk at

(79) Wittung-Stafshede, P.; Hill, M. G.; Gomez, E.; Di Bilio, A. J.; Karlsson, B. G.; Leckner, J.; Winkler, J. R.; Gray, H. B.; Malmström, B. G. *J. Biol. Inorg. Chem.* **1998**, *3*, 367−370.
(80) Wittung-Stafshede, P.; Gomez, E.; Ohman, A.; Aasa, R.; Villahermosa, R. M.; Leckner, J.; Karlsson, B. G.; Sanders, D.; Fee, J. A.; Winkler, J. R.; Malmström, B. G.; Gray, H. B.; Hill, M. G. *Biochim. Biophys. Acta* **1998**, *1388*, 437−443.
(81) Blackburn, N. J.; Ralle, M.; Gomez, E.; Hill, M. G.; Pastuszyn, A.; Sanders, D.; Fee, J. A. *Biochemistry* **1999**, *38*, 7075−7084.
(82) Fernandez, C. O.; Cricco, J. A.; Slutter, C. E.; Richards, J. H.; Gray, H. B.; Vila, A. J. *J. Am. Chem. Soc.* **2001**, *123*, 11678−11685.

the University of Illinois U-C for the use of a potentiostat and faraday cage, and Dr. Mark J. Nilges of the NIH Illinois EPR Research Center (IERC) for assistance with the Q-band EPR spectrometer and for providing the EPR simulation program. We gratefully acknowledge the use of facilities at the Stanford Synchrotron Radiation Laboratory, which is supported by the National Institutes of Health Biomedical Research Technology Program, Division of Research Resources, and by the U.S. Department of Energy, Basic Energy Sciences (BES) and Office of Biological and Environmental Research (OBER).

Supporting Information Available: Fourier transforms and EXAFS spectra for Met121Nle variant of azurin produced by EPL (PDF). This material is available free of charge via the Internet at http://pubs.acs.org.

JA029699U